TECHNICAL REPORT

September 15, 1971

ARPA order number: 1479

Program code number: NR 012-133

Contract number: N00014-67-A-0097-0008

Modification number: 05

Amount of Contract: $50,000

Contract Expiration: June 30, 1972

Yale University

New Haven, Connecticut 06520

Principal Investigator

George J. Schulz
Mason Laboratory
Yale University
New Haven, Connecticut
Phone 203/436-3046

Title: THREE-BODY ATTACHMENT IN O_2 USING ELECTRON BEAMS

by D. Spence and G. J. Schulz

The views and conclusions contained in this document are those of the authors and should not be interpreted as representing the official policies of ARPA.

Security Classification

DOCUMENT CONTROL DATA - R & D

Security classification of title, body of abstract and indexing annotation must be entered when the overall report is classified)

YALE UNIVERSITY New Haven, Connecticut	2a. REPORT SECURITY CLASSIFICATION Unclassified 2b. GROUP

3. REPORT TITLE

THREE-BODY ATTACHMENT IN O_2 USING ELECTRON BEAMS

4. DESCRIPTIVE NOTES (Type of report and inclusive dates)

Technical Report

5. AUTHOR(S) (First name, middle initial, last name)

George J. Schulz
David Spence

6. REPORT DATE	7a. TOTAL NO. OF PAGES	7b. NO. OF REFS
September 15, 1971	22 + 9 figures	33

8a. CONTRACT OR GRANT NO.	9a. ORIGINATOR'S REPORT NUMBER(S)
N00014-67-A-0097-0008 b. PROJECT NO.	
c.	9b. OTHER REPORT NO(S) (Any other numbers that may be assigned this report)
d.	

10. DISTRIBUTION STATEMENT

Distribution of this document is unlimited.

11. SUPPLEMENTARY NOTES	12. SPONSORING MILITARY ACTIVITY
	ARPA

13. ABSTRACT

The three-body attachment reaction in O_2, $e + 2O_2 \rightarrow O_2^- + O_2$, is studied by electron beam techniques. Whereas swarm experiments show a smooth variation of the attachment coefficient with energy, the present electron beam experiment shows pronounced structure. The peaks of this structure occur at the positions of the vibrational levels of the O_2^- system, which serve as compound states and have been identified in a previous experiment. These compound states dominate the low-energy cross sections in O_2. They can decay by autodetachment, thus accounting for the bulk of the vibrational cross sections in O_2 at low energy; alternatively, they can be stabilized by a subsequent collision, thus leading to the formation of stable O_2^-. Thus we establish clearly that three-body attachment in O_2 is a two-stage process and that the intermediate is a vibrationally existed state of O_2^-. We also obtain the temperature dependence of the three-body attachment at higher pressures. The experimental observations are in excellent agreement with the theory of Chapman and Herzenberg.

DD FORM 1473 (PAGE 1)

0102 014 6600

Security Classification

14 KEY WORDS	LINK A		LINK B		LINK C	
	ROLE	WT	ROLE	WT	ROLE	WT
Attachment						
Negative ions						
Electron beams						
Oxygen						
Temperature dependence						
Three-body						

THREE-BODY ATTACHMENT IN O_2 USING ELECTRON BEAMS[†]

D. Spence and G. J. Schulz

Mason Laboratory, Yale University, New Haven, Conn. 06520

The three-body attachment reaction in O_2, $e + 2O_2 \rightarrow O_2^- + O_2$, is studied by electron beam techniques. Whereas swarm experiments show a smooth variation of the attachment coefficient with energy, the present electron beam experiment shows pronounced structure. The peaks of this structure occur at the positions of the vibrational levels of the O_2^- system, which serve as compound states and have been identified in a previous experiment. These compound states dominate the low-energy cross sections in O_2. They can decay by autodetachment, thus accounting for the bulk of the vibrational cross sections in O_2 at low energy; alternatively, they can be stabilized by a subsequent collision, thus leading to the formation of stable O_2^-. Thus we establish clearly that three-body attachment in O_2 is a two-stage process and that the intermediate is a vibrationally existed state of O_2^-. We also obtain the temperature dependence of the three-body attachment at higher pressures. The experimental observations are in excellent agreement with the theory of Chapman and Herzenberg.

I. INTRODUCTION

The capture of free electrons by molecular oxygen leading to the formation of stable molecular negative ions is one of the more important processes leading to removal of thermal electrons from the upper atmosphere. Indeed, in certain atmospheric plasmas, this is the dominant electron removal mechanism, and a complete understanding of this mechanism is of interest.

The attachment of low-energy (0-1 eV) electrons to molecular oxygen has been the subject of intensive study over a period of forty years, and a wealth of experimental and theoretical data is available. However, it is only in recent years that an understanding of the attachment process has come about.[1-4]

In the present experiments we study the electron attachment process at low electron energies (0-1 eV) over a wide range of target gas temperatures using monoenergetic electrons. By the use of a monoenergetic electron beam we are able to study details of the attachment process hitherto unobservable. The use of high target gas temperatures enables us to study the thermal effect on the attachment process. This latter consideration is of great importance, as molecular oxygen in the upper atmosphere is often at a high kinetic temperature and may be in a state of vibrational excitation.

Previous data and proposed mechanisms for electron attachment are reviewed in Section II. In Sections III and IV we discuss the apparatus and the acquisition of data. The experimental results are presented in section V together with a comparison of the latest theoretical work.

II. SUMMARY OF PREVIOUS WORK

It is now well known that electron attachment to molecular oxygen at low incident electron energies leading to the formation of O_2^- is a three-body process, which proceeds in two stages. In the first stage, the electron is captured by the molecule into a vibrationally excited temporary negative ion state, sometimes called a compound or resonant state; i.e., $O_2 + e \rightarrow O_2^{-*}$. This excited molecular ion may subsequently autoionize into a free electron and a neutral molecule which may be left in a vibrationally excited state $O_2^{-*} \rightarrow O_2(v) + e$. Alternatively, the excess energy of the molecular ion may be removed in a collision with a third body, which in the case of pure oxygen is another O_2 molecule; i.e., $O_2^{-*} + O_2 \rightarrow O_2^-$ (stable) $+ O_2 +$ KE. Such a two-stage process was first proposed by Bloch and Bradbury[5] in 1935. They assumed that the potential energy curves of the neutral molecule and the molecular ion differed only in a vertical displacement, thus implying that the vibrational spacings of the neutral molecule and molecular ion are identical. This restriction implies that electron capture can only occur by non-adiabatic coupling involving the nuclear velocities. If electron capture occurs through non-adiabatic coupling, only the first vibrationally excited state of the molecular ion can be excited with a high probability. This level must be above the ground state of O_2, so the electron affinity of molecular oxygen cannot exceed the vibrational spacing of the neutral molecule. The Bloch-Bradbury theory further implies that electron attachment should occur only at a unique value of incident electron energy, and the energy spectrum of O_2^- should consist of a single sharp line.

Many early experiments[6,7,8] indicated that the attachment process exhibited a two-body pressure dependence. Because of this evidence, Bloch and Bradbury had to assume that the lifetime of the excited state of O_2^- involved was much larger than the time between molecular collisions so that most of the excited molecular ions would become stabilized.

In 1962 Chanin, Phelps and Biondi[1] showed conclusively from swarm experiments that at low electron energies attachment exhibits a three-body pressure dependence at least up to 150 mm; i.e., O_2^- production varies quadratically as the gas pressure. This was verified by Schulz[9] using an electron beam technique. From these measurements Chanin et al. estimated that the lifetimes of the excited O_2^- state was between 10^{-10} and 5×10^{-12} sec, much less than assumed in the Bloch-Bradbury theory. Further, Pack and Phelps [3] have determined the electron affinity of O_2 to be 0.43 ± 0.02 eV. This value of the electron affinity has recently been confirmed by Cellota et al.[10] using a photoionization technique and by Compton[11] et al. using a charge exchange method. This value of the electron affinity implies that vibrational levels of the O_2^- state higher than v=1 must play a role in the attachment mechanism, destroying the simple Bloch-Bradbury model of a vertical displacement of the potential curves.

In a recent theoretical treatment of three-body attachment in oxygen, Herzenberg[12] treats the problem differently in two respects. 1) He removes the unphysical restriction that the spacial separations of the nuclei are the same at the minima of the potential curves in the ion and neutral molecule. The removal of this restriction makes possible the capture of the electron into more than only the first vibrational level of the ion through the much simpler mechanism of adiabatic coupling. 2) Herzenberg describes the initial electron capture process in terms of a Breit-Wigner[13] formula. The Breit-Wigner formula

is a general expression for the energy dependence of a cross section in the region of a resonant or temporary negative ion state. The use of the Breit-Wigner formula avoids a detailed description of the actual capture mechanism, thus simplifying the problem.

In order to calculate the rate of formation of stable O_2^-, it is necessary to take the product of 3 terms; viz. 1) the rate of formation of the excited negative ion states, 2) the probability that an ion will make a collision with a neutral particle before decaying, and 3) the probability that such a collision will be a stabilizing one. Herzenberg treats the collision of the ion and molecule as being one of the spiralling type first described by Langevin. Herzenberg finds that the rate constant K can be written as [14]

$$(1)\quad K(E) = (8/3)\ (\pi^3 \hbar^2/m)\ (\alpha e^2/M)^{\frac{1}{2}}\ \xi\ \Sigma_{v'}\ f(E^{v'}, E)\ \lambda\!\!\!^{-}(E^{v'})\ (\Gamma_v^{v'}/\Gamma^{v'})$$

The symbol v' refers to a vibrational state of O_2^-, and v designates a vibrational state of O_2. The term $\Gamma_v^{v'}$ is the entry width from state v of O_2 to state v' of O_2^-, and $\Gamma^{v'}$ is the total width of state v'. The term $(\alpha e^2/M)^{\frac{1}{2}}$ describes the long-range polarization interaction between the ion and molecule where α is the polarizability and ξ is the probability that the collision of O_2 and O_2^{-*} will be a stabilizing one. The reduced wavelength of the incident electron in the region of a resonance v' is $\lambda\!\!\!^{-}(E^{v'})$ and $f(E^{v'},E)$ is the value of the incident electron energy distribution at the resonance energy $E^{v'}$ where the mean electron energy is E. From theoretical considerations, Herzenberg concludes that ξ is of the order of unity for the low-lying resonances.

The vibrational spacings of the O_2^- system are now well established, [15 - 18] and the vibrational levels of the O_2^- system have been accurately fixed with respect to those of the neutral molecule.[16,17] The lifetimes of the lowest few levels of O_2^{-*} above v=0 of O_2 are believed to be of the order of 10^{-10} sec.[12] Further,

it is known that the separation of nuclei in the ion and molecule are different at the minima of the potential curves.[10,12,19] From this evidence one would expect the rate constant for O_2^- production to consist of a series of spikes, which occur at the energies of the vibrational levels of O_2^- above v=0 of the neutral molecule. That these spikes have never previously been observed is hardly surprising in view of the narrow energy distribution necessary to resolve them (which usually implies small primary electron beam current) combined with the need to operate at relatively high pressures.

III. APPARATUS

Figure 1 is a schematic diagram of the experimental tube used in the present experiments. This tube has been described in detail previously[20] and only a brief description will be given here.

Electrons are emitted from a directly-heated thoria-coated iridium filament, and the effective width of the electron energy distribution is reduced to about 80-100 meV by the retarding potential difference method.[21] The electron beam is confined by a magnetic field, which in the present experiments is about 1000 G.

The collision chamber consists of an iridium cylinder which can be heated by the passage of a direct current. Inside the collision chamber are mounted a pair of parallel iridium plates which serve as collectors. The experimental tube, with the exception of the iridium parts, are gold plated to minimize contact potential differences. After baking at 300°C for 24 hours the background pressure in the vacuum system is of the order of 5×10^{-9} torr.

Negative ions produced in the collision chamber are extracted by maintaining an electric field between the parallel plate collectors. The collected current is measured by a vibrating reed electrometer and stored in

a multichannel analyzer. The potential on the retarding electrode of the electron gun and the add/subtract current of the multichannel analyzer are switched at the beginning of alternate scans in a mode similar to that described by Chantry[22] to give automatic data recording. The primary electron beam current is typically $1.0 - 5.0 \cdot 10^{-9}$ A.

IV. ACQUISITION OF DATA

The rate constant K for the attachment of electrons to O_2 in a three-body process may be written as $K = (Q_{eff}\ v/N)$. Here, Q_{eff} is an effective cross section for the production of stable O_2^- governed by the relation $i(O_2^-) = i_o\ NQ_{eff}\ L$, where N is the gas density, L is the length of the chamber, i_o is the primary electron current, $i(O_2^-)$ is the negative ion current and v is the electron velocity. In the present apparatus there is no provision for direct measurement of the gas density in the collision chamber. The average gas density along the collision path is calculated from measurements of positive and negative ions produced by known electron currents, the relevant ionization [23] and dissociative attachment[20] cross sections being known. The density is also measured by electron beam attenuation experiments. The density data obtained in this way are plotted against the background pressure in the vacuum chamber. The background pressure and the density in the collision chamber are found to be directly related over a range of five orders of magnitude in the background pressure, when slight corrections for multiple electron scattering[24] in the collision chamber are made at the highest gas densities. The ratio of gas density in the collision chamber to that in the background is about 200.

The magnitude of Q_{eff} is determined by measuring the O_2^- current at low incident electron energy, and normalizing this signal against the O^- current produced from dissociative attachment in oxygen at 6.7 eV, using the

same target gas density and electron beam current. The rate constant for O_2^- production peaks at about 0.1 eV, whereas the dissociative attachment cross section for production of O^- peaks at an incident electron energy of 6.7 eV and has been measured in many independent experiments to be[25] 1.30 ± 0.05 $10^{-18}cm^2$. Since the rate of production of O_2^- varies quadratically with target gas density and that for O^- varies linearly, the ratio of the two currents should vary linearly with density. Figure 2 shows a plot of the ratio of the negative ion current at 0.1 eV to negative ion current at 6.7 eV. The plot is seen to be linear over a wide range of target gas densities, indicating that the peak at 0.1 eV does vary quadratically with the gas density and is indeed O_2^-. Deviations from linearity occur when the target gas density becomes greater than about $4 \times 10^{15}cm^{-3}$. Above this density the collision number, NQL, (where N is the gas density, Q the elastic cross section for electrons, and L the collision chamber length) becomes significantly greater than one. Under such conditions a significant fraction of electrons make elastic collisions in the collision chamber, thus effectively increasing the path length over which the electrons may collide to form a negative ion. The theory of electron-gas collisions at intermediate and high gas pressures has been developed by Chantry, Phelps and Schulz[24]. The equivalent length factors g_1 and g_2 for the production of O_2^- and O^- at 0.1 and 6.7 eV respectively are obtained from Fig. 7 of Ref. 24. The elastic collision number is calculated using the elastic scattering cross section of Hake and Phelps[26] who obtained $Q_{elastic} = 4.4\ 10^{-16}$ cm^2 at 0.1 eV and $Q_{elastic} = 6.4\ 10^{-16}\ cm^2$ at 6.7 eV. The ratio g_1/g_2 is plotted as the dashed curve in Fig. 3 and is normalized to the linear part of the experimental curve. Although this theory indicates the correct density at which the deviations from linearity occur, the experimental and theoretical points do not exactly coincide. The equivalent length factors are dependent

upon the ratio 1/m = inelastic cross section/elastic cross section. Chantry, Phelps and Schulz plot the equivalent length factos for 1/m = 0, 0.01 and 0.10. In estimating g_2 for O^- production at 6.7 eV we have used 1/m = 0.01. The true value of 1/m at this energy is 0.025. This results in a slight overestimate of g_2 and a consequent understimate in the ratio g_1/g_2, causing divergence between the experimental and calculated curves. The calculations do,however, explain qualitatively the divergence from linearity.

Negative ions are collected with a draw-out field sufficient to collect all the ions formed. Particular care is taken that no potential well occurs in the collision chamber when collecting the O_2^- current. Such a potential well would result in the collection of elastically and inelastically scattered ("trapped")[27] electrons in addition to the true O_2^- signal. The linearity of the plot in Fig.2 is an indication that no such potential well exists. Effective cross sections measured with beam currents of 1-5 x 10^{-9} A are the same as those measured with beams of 3 x 10^{-8} A, indicating that any space charge effects are negligible. The O_2^- ions formed have very little kinetic energy and quite low draw-out fields are sufficient to ensure saturation. Because of thelow energy of the O_2^- ions, care must be taken that the Larmor radius of the ions in the magnetic field is not less than the distance of the collection plate from the point of formation of the ions. If this were the case, O_2^- ions would be lost to the side walls of the collision chamber. The effective cross section for electron attachment to O_2 is found to be independent of the magnetic field for values between 500-1500 G. If the magnetic field is increased above 1500 G, a rapid decrease in the O_2^- signal occurs.

V. RESULTS

Figure 3 is a recorder tracing of the O_2^- current as a function of electron energy. This trace represents the signal produced by the averaging of 256 successive electron energy scans in the multichannel analyzer. The vibrational energy levels of the O_2^- system with respect to the ground vibrational state of the neutral molecule have been determined previously[16] and are shown at the top of the figure. The experimental peaks in the effective O_2^- cross section are seen to occur whenever the incident electron energy coincides with a vibrational level of the negative ion system. The lifetimes of the lowest levels of the O_2^{-*} system above $v'=4$ are long (10^{-10} sec) and hence the widths of the levels are narrow, about 10 μV. Consequently the effective cross section for O_2^- production should consist of a series of spikes 10 μV wide. The observed widths and the overlapping of the peaks in the present experiments are due entirely to the energy spread of the primary electron beam.

The rate constant in arbitrary units is calculated from the effective cross section of Fig. 3 by multiplying it by $E^{1/2}$ where E is the incident electron energy. The rate constant calculated in this way is plotted in Fig. 4. Also plotted in Fig. 4 is the maximum theoretical rate constant for three-body attachment calculated by Chapman and Herzenberg[4,14] for a Gaussian electron energy distribution with a half-width of 110 mV. The experimental points have been normalized to the theoretical points at the second peak in the rate constant. The maximum theoretical rate constant is calculated from Eq.1 by assuming that ξ (the probability that a collision between O_2^{-*} and O_2 will be a stabilizing one) is unity and independent of energy. In the calculations, $\Gamma_v^{v'}/\Gamma^{v'}$, the probability that an excited state v' of the ion will decay into a given state v of the molecule is obtained theoretically, and the resonance energies $E^{v'}$ are obtained from experimental data. The agreement between the theory and the

present experiment is seen to be particularly good at low energy; small deviations occur above about 0.6 eV. As pointed out to us by Herzenberg, this deviation could result from a variation of the coefficient ξ with energy. One would expect that at higher incident energies (corresponding to the excitation of high levels of the O_2^- system), stabilization is more difficult because the O_2^{-*} system may still end up in an autoionizing state, and only particularly favorable events will lead to the formation of stable O_2^-. On the other hand, when the incident electron produces O_2^- in the 4th vibrational state, most collisions are expected to be of the stabilizing kind. This effect, leading to a decrease in the stabilization coefficient with energy, is not included in the theory and could cause the discrepancy of Fig. 4

The present data are compared with the swarm experiments of Pack and Phelps[3] in Fig. 5 Here we have normalized our data to those of Pack and Phelps[3] at the first peak. Figure 5 shows that although the electron energy spread in the swarm experiments is too large to resolve any structure, the swarm data do follow very closely the envelope of the present data. The swarm data are higher at higher energy, compared to the electron beam data because the electron energy distributions in the two types of experiment differ considerably. In a swarm experiment the electron energy spread is approximately equal to half the mean electron energy.

The absolute value of the rate constant is calculated from the data of Fig. 4 combined with Fig. 3, the cross section for O^-/O_2 production at 6.7 eV being known. The absolute rate constant at the peak which occurs at about 0.09 eV is found to be $(5.6 \pm 1.3) \times 10^{-30} cm^6$ in the present work. This value is in very good agreement with that of Chanin, Phelps and Biondi,[1] and of Pack and Phelps[3] who give a value of $4.8 \times 10^{-30} cm^6/sec$. Both these experimental values are also in very good agreement with the maximum theoretical value of

$4.7 \times 10^{-30} cm^6/sec.$ calculated[4] for an electron energy distribution of 110 meV. The agreement between the experimental and theoretical value indicates that for at least the low vibrational levels of O_2^-, ξ the probability that a collision will be a stabilizing one, is indeed very close to unity. To obtain better agreement between theory and experiment at the higher energies would entail very much more complicated calculations.

VI. TEMPERATURE DEPENDENCE

For measurements of the rate constant at high gas temperatures, the collision chamber is heated by passing a direct current through it. For a fixed rate of gas flow through the system, the density in the collision chamber falls as $T^{-1/2}$. For a fixed electron current, the flow rate of the gas is increased until the O^- current at 6.7 eV is the same as that produced at room temperature. This insures that the gas density in the collision region remains constant as the gas temperature is increased. The cross section for O^-/O_2 production at 6.7 eV is known to be essentially independent of gas temperature[20,28] in the range 300-1000°K. Figure 5 shows a comparison of the present data and those of swarm experiments[1,3] at room temperature and at 500°K. Although the swarm data fits the envelope of the present data very well at both temperatures, a larger temperature dependence of the first peak is indicated by the swarm experiments than in the present data. As mentioned earlier, the measured shape of the rate constant is a convolution of the electron energy spread with a set of narrow spikes, whose spacing is equal to the vibrational spacings of the negative ion system. Consequently, the peak height of the measured signal will be critically dependent on the electron energy spread.[29]

In the present experiments only single collisions between the incident electrons and the target molecule occur and thus the incident electron energy spread is not altered as the gas temperature increases. In swarm experiments the electrons make many collisions and the energy spread is increased by the thermal motions of the target gas. The increase in energy spread will therefore be greater at higher gas temperatures, leading to a decrease in the measured value of K at the peak. This effect may partially explain the discrepancy between the present data and those obtained from swarms.

Figure 6 shows a plot of the temperature dependence of the rate constant at the first peak. Also shown in Fig. 6 are the results of Pack and Phelps.[3] The present data are normalized to those of Pack and Phelps at 0.09 eV and 300°K. In the present experiments it is not possible to extend measurements much above 750°K, because thermal drifts in the feedthrough insulators of the collision chamber made long term averaging of the very small O_2^- currents impossible.[30]

Both the present and the swarm data of Fig. 5 indicate that the temperature dependence of the rate constant becomes less pronounced as the energy increases. This is illustrated more clearly in Fig. 7 where we have plotted the fractional change in the rate constant as a function of gas temperature at electron energies of 0.09, 0.34 and 0.57 eV. These electron energies correspond to the energies of the v'=4, 6 and 8 vibrational states of O_2^-. The reactions which can occur when an O_2^{-*} ion collides with a neutral O_2 molecule are:

$$O_2^{-*} + O_2 \rightarrow O_2^- + O_2 + \text{energy} \qquad \text{(i)}$$

$$O_2^{-*} + O_2 \rightarrow O_2^{-*} + O_2 + \text{energy} \qquad \text{(ii)}$$

$$O_2^{-*} + O_2 \rightarrow O_2 + O_2 + e \qquad \text{(iii)}$$

Reaction (i) is the stabilization process in which either O_2^- or O_2 may be left excited, provided only that the negative ion is stable against emission of an electron. Reaction (ii) is elastic or inelastic scattering leaving O_2^{-*} with sufficient energy to emit an electron. Reaction (iii) is electron detachment, and can be a powerful reaction when the collision partners have sufficient energy.[12]

VII. HIGH PRESSURE MEASUREMENTS

At target gas densities greater than about $10^{15}cm^{-3}$, a large broad peak centered at about 0.6 eV incident electron energy is seen to appear on the effective cross section for O_2^- production. This broad peak, illustrated in Fig. 8 increases at a rate greater than the square of the gas density and has previously been observed by Schulz[31] in 1961 in a total ion collection apparatus, and by Compton[32] in an apparatus with mass analysis. The latter study definitely identifies the ion involved as being O_2^-. Such a peak is not observed in swarm experiments even at 100 times higher gas densities. Measurements of the ratio of the magnitude of the broad peak at 0.6 eV to the magnitude of the peak at about 0.1 eV exhibit a linear pressure dependence, as shown in Fig. 9. Since we have previously shown that the peak at 0.1 eV varies as N^2, Fig. 9 indicates that the peak at 0.6 eV varies as N^3. Measurements show that the ratio (peak 0.6 eV/peak 0.1 eV) is independent of the incident electron current.

There are at least two possible explanations for this broad peak: (1) Oxygen at room temperature is able to form dimers, i.e., $O_2 + O_2 \rightarrow O_4$. The rate constant of such a process is of course dependent on N^2. It is possible that an oxygen dimer so formed would undergo dissociative attachment by electron impact, leaving the molecular ion vibrationally excited, i.e., $O_4 + e \rightarrow O_2 + O_2^{-*}$. This excited molecular ion could then be stabilized by a collision with another O_2 molecule. Combinations of the two above processes would yield an O_2^- signal which varies as N^3 consistent with our observations. However, such a process, if it exists, should be observed in swarm experiments, which is not the case. The binding energy of O_4 is very small and if the observed peak at 0.6 eV were due to the above process, it would disappear on heating the gas by a few hundred degrees by removing any O_4. It is found, however, that the magnitude of the O_2^- peak eV does not strongly depend on the gas temperature. This fact seems to rule out dimers as a cause for the 0.6 eV peak.

(2) If the incident electrons lose most of their energy in an inelastic collision with the target gas, they will then be able to participate in the usual three-body attachment process at low electron energy. Such a process can occur when the gas density is high enough to cause multiple scattering of the electrons and the O_2^- current produced will then vary as N^3.

We have previously shown[16] that the vibrational excitation cross section of molecular oxygen consists of a series of spikes which are coincident in energy with the resonances (vibrational levels) in the negative ion system. When an electron with initial energy, V_o, excites a vibrational state of oxygen via one of these negative ion states, the electron is left with an energy $E = (V_o - V_x)$, where V_x is the energy of the final vibrational state of the neutral molecule. Using the data of Ref 16, Chapman and Herzenberg[4] have extended to

higher energies the vibrational excitation cross section for v = 1, 2 and 3 of O_2. Their data show that the envelope of the spikes for the v = 1 cross section has a maximum at about 0.6 eV, and for v = 2 at about 0.9 eV. This finding is in good agreement with the recently reported results of Linder and Schmidt[17] who observe experimentally that the envelope of the spikes for v = 1 peaks around 0.6 eV. We have used the data of Chapman and Herzenberg to calculate the relative fraction of the incident electrons which suffer a particular energy loss, i.e. the relative fractions of electrons whose final energy is ($V_o - V_x$). The relative current of O_2^- produced in a three-body collision by these electrons which have energy $V_o - V_x$ is calculated by use of Fig. 3. The calculated current of O_2^- produced by electrons which have suffered this energy loss mechanism is shown in Fig. 8 by the dashed curve. This figure shows that the process described above predicts very well the observed shape of the effective O_2^- cross section at high densities, and satisfies the required pressure dependence.

The process which we invoke for the explanation of the 0.6 eV peak in Fig. 8 is entirely analogous to the process described by Chantry[33] to explain the peaks which occur in the dissociative attachment cross section in molecular oxygen at 15 eV. In dissociative attachment the observed signal is proportional to N^2 whereas in our case it is proportional to N^3.

The above mechanism does not produce a peak at 0.6 eV in swarm experiments. In an electron beam experiment the electrons in the collision chamber are not subject to any accelerating electric field along their path. Consequently, once an electron has lost energy in an inelastic collision, it may fall into an energy range where three-body attachment is at its peak. In a swarm experiment the electrons are subject to a uniform accelerating field and thus continually gain energy from the field and lose energy in inelastic collision. After the first few hundred collisions the electron energy distribution is independent of position.

VIII. DISCUSSION

We have pointed out previously that electron collision processes at low energies in diatomic molecules are dominated by the existence of the compound states. This paper points out that even three-body attachment processes must be interpreted in terms of these compound states. The parameters of the compound state in O_2 are now well enough known so that a meaningful theoretical treatment is possible. This task has been recently completed by Chapman and Herzenberg, who could calculate both the vibrational cross sections and three-body attachment from the parameters of the compound state.

IX. ACKNOWLEDGEMENT

The authors are indebted to A. Herzenberg and to C. Chapman for frequent illuminating discussions of the theory and to A. V. Phelps for his comments.

REFERENCES

* This work was supported by ARPA through ONR and by DASA through AROD.

1. L. M. Chanin, A. V. Phelps and M. A. Biondi, Phys. Rev. 128, 219, (1962).

2. R. Grunberg, Z. Naturforsch 24a, 1039, (1969).

3. J. L. Pack and A. V. Phelps, J. Chem. Phys. 44, 1870, (1966).

4. C. Chapman and A. Herzenberg, (To be published).

5. F. Bloch and N. Bradbury, Phys. Rev. 48, 689, (1935).

6. N. E. Bradbury, Phys. Rev. 48, 883, (1933).

7. A. Doehring, Z. Naturforsch 7a, 253, (1952).

8. P. Herreng, Cahiers Phys. 38, 7, (1952).

9. G. J. Schulz, Bull. Am. Phys. Soc. 6, 387, (1961).

10. R. J. Celotta, R. A. Bennett, J. L. Hall, M. W. Siegel and J. Levine, Bull. Am. Phys. Soc. II, 15, 1515, (1970). See also R. J. Celotta, R. A. Bennett and J. L. Hall in Abstracts of the Seventh International Conference on the Physics of Electronic and Atomic Collisions, Amsterdam, 1971, (North Holland Publishing Co., Amsterdam, 1971), page 179.

11. R. W. Compton, Chem. Phys. Lett. 9, 529, (1971).

12. A. Herzenberg, J. Chem. Phys. 51, 4943, (1969).

13. G. Breit and E. Wigner, Phys. Rev. 49, 519, (1936). See also: J. M. Blatt and V. F. Weisskopf, Theoretical Nuclear Physics, (John Wiley and Sons, Inc., New York, 1952, page 392).

14. See Ref. 4 and also C. Chapman, Ph.D. Thesis, University of Manchester, 1970.

15. M. J. W. Boness and J. B. Hasted, Phys. Lett. 21, 526, (1966).

16. D. Spence and G. J. Schulz, Phys. Rev. A2, 1802, (1970). The extrapolated spacing $v = 0 \rightarrow v = 1$ is found to be 132 meV and the anharmonicity, $\hbar\omega_e x_e = 1.5$ meV.

17. F. Linder and H. Schmidt in Abstracts of the Seventh International Conference on the Physics of Electronic and Atomic Collisions, Amsterdam, 1971, (North Holland Publishing Co., Amsterdam, 1971), page 336. Linder and Schmidt find the extrapolated spacing for $v = 0 \rightarrow v = 1$ for O_2^- to be 135 meV and the anharmonicity $\hbar\omega_e x_e = 1$ meV. It should be noted that this finding results from the spacings of the structure in the vibrational cross section, which is not afflicted by interference phenomena. This method should, in principle, be very reliable. We also note that the absolute magnitude of the vibrational cross sections measured by Linder and Schmidt is an order of magnitude larger than that measured in Reference 16 using the trapped-electron method. Although we do not know the cause for the discrepancy, the experiment of Linder and Schmidt appears to us convincing.

18. R. L. Gray, H. H. Haselton, D. Krause, Jr. and E. A. Soltysik in Abstracts of the Seventh International Conference on the Physics of Electronic and Atomic Collisions, Amsterdam, 1971, (North Holland Publishing Co., Amsterdam, 1971), page 347. Gray et al find an extrapolated spacing for $v = 0 \rightarrow v = 1$ for O_2^- about 140 meV and an anharmonicity of $\hbar\omega_e x_e = 1.5$ meV.

19. M. J. W. Boness and G. J. Schulz, Phys. Rev. A2, 2182, (1970).

20. D. Spence and G. J. Schulz, Phys. Rev. 188, 280, (1969).

21. R. E. Fox, W. M. Hickam, D. J. Grove and T. Kjeldaas, Rev. Sci. Instr. 26, 1101, (1955).

22. P. J. Chantry, Rev. Sci. Instr. 40, 884, (1969).

23. D. Rapp and P. Englander-Golden, J. Chem. Phys. 43, 1464, (1965).

24. P. J. Chantry, A. V. Phelps and G. J. Schulz, Phys. Rev. 152, 81, (1966).

25. For a review see Ref. 20.

26. R. D. Hake and A. V. Phelps, Phys. Rev. 158, 70, (1967).

27. G. J. Schulz, Phys. Rev. 112, 150, (1958); 1141, (1959).

28. W. R. Henderson, W. L. Fite, and R. T. Brackmann, Phys. Rev. 183, 157, (1969).

29. Calculations by Chapman and Herzenberg show that for an electron energy distribution 70 meV wide, the spikes in the rate constant are entirely resolved, while for a distribution slightly more than double this width, 150 meV, any structure is completely smeared out, producing an envelope similar to that obtained by Pack and Phelps. Further, according to these calculations, the first peak of K_{max} is reduced from 7.1 10^{-30} cm^6/sec. for 70 meV energy spread, to 3.9 x 10^{-30} cm^6/sec. for 150 meV energy spread, illustrating the sensitivity of the measured value on the incident electron energy spread.

30. The same apparatus has been used to measure the temperature dependence of other collision cross sections up to temperatures as high as 1300°K. However, in these cases the cross sections were larger and no signal averaging was required.

31. G. J. Schulz (unpublished).

32. R. N. Compton, (Private communication).

33. P. J. Chantry, J. Chem. Phys. 55, 1851 (1971)

FIGURE CAPTIONS

Fig. 1: Schematic diagram of the apparatus.

Fig. 2: Ratio of the O_2^- current at 0.1 eV to the O^- current at 6.7 eV, plotted as a function of target gas density N. The linear plot shows that the O_2^- signal is dependent upon N^2. All measurements of the rate constant K were made at a target gas density on the linear part of this plot.

Fig. 3: The effective [illegible]-section for production of stable O_2^- as a function of incident electron energy. The vibrational spacings of the O_2^- system which were obtained in previous experiments are indicated at the top of the figure.

Fig. 4: The three-body rate constant K for production of O_2^- in pure O_2, in comparison with the theoretical data of Chapman and Herzenberg, plotted as a function of incident electron energy. The present data and those of Chapman and Herzenberg are normalized at the second peak. The vibrational spacing of the O_2^- system are indicated at the top of the figure.

Fig. 5: The three-body rate constant K for production of O_2^- in pure O_2 at 300°K and 500°K, normalized to the experimental data of Pack and Phelps at the peak of their 300°K curve. The vibrational spacings of the O_2 system are indicated at the top of the figure.

Fig. 6: Temperature dependence of the peak at 0.09 eV in the rate constant K for production of O_2^- in pure O_2, in comparison with the experiment of Pack and Phelps. The present data are normalized to those of Pack and Phelps at 300°K.

Fig. 7: Fractional variation of the three-body rate constant as a function of target gas temperature. The data, which are plotted for three incident electron energies, show that the rate constant is less dependent on target gas temperature at higher incident electron energy.

Fig. 8: Effective cross-section for O_2^- production in pure O_2 at high target gas density as a function of incident electron energy. The data show a large "hump" centered around 0.6 eV. The lower (dashed) curve shows the calculated cross-section for O_2^- production by electrons which have lost energy in making an inelastic collision. The vibrational spacings of the O_2^- system are indicated at the top of the figure.

Fig. 9: Ratio of the O_2^- peak at 0.6 eV to the O_2^- peak at 0.1 eV. This plot indicates that the "hump" at 0.6 eV in Fig 9 is dependent on the cube of the target gas density.

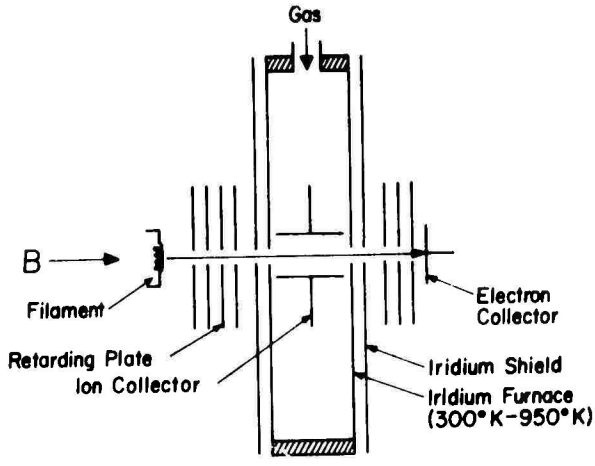

DIAGRAM of APPARATUS

FIG. 1

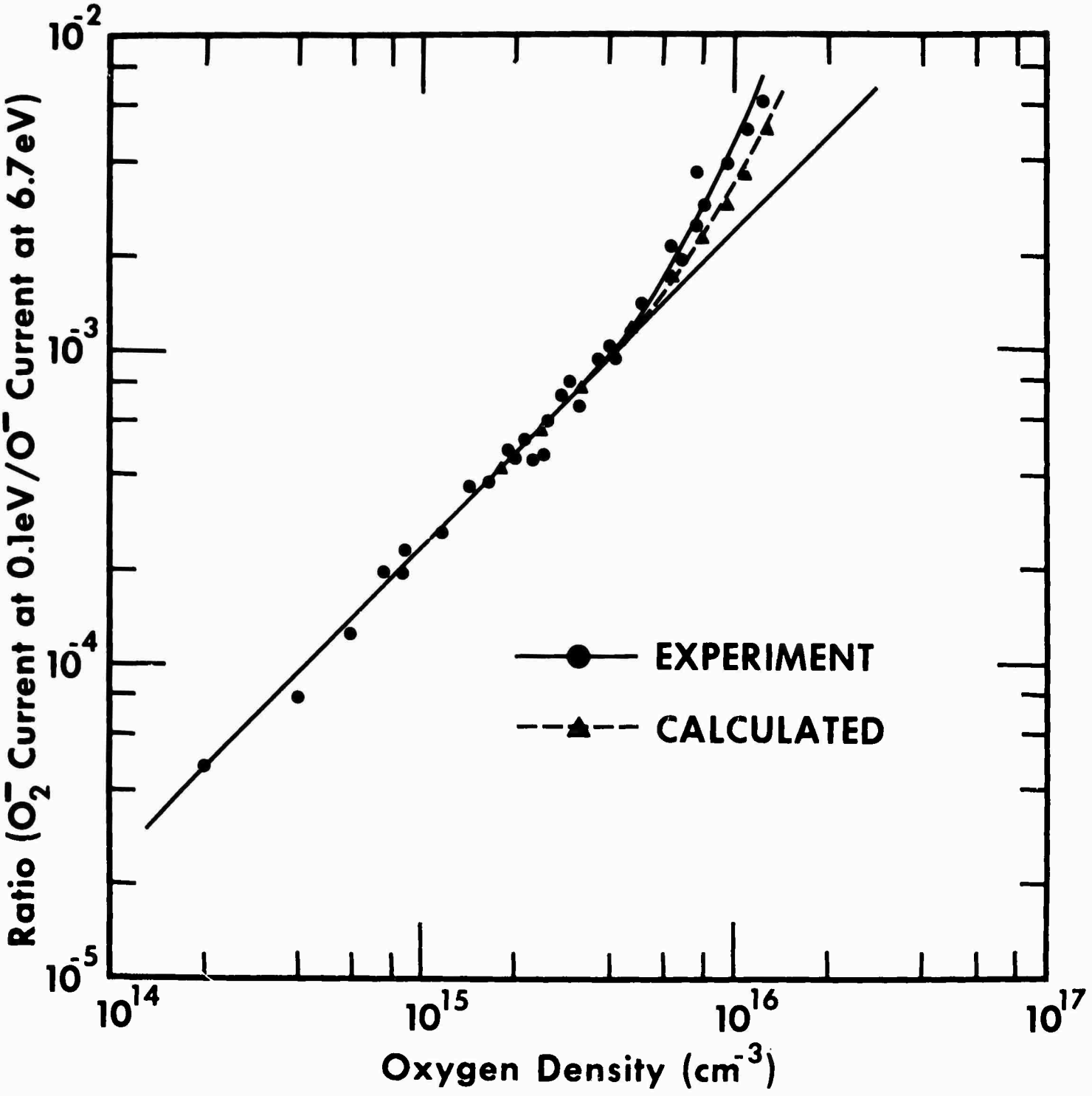

PRESSURE DEPENDENCE OF O_2^-/O^- AT 300°K

FIG. 2

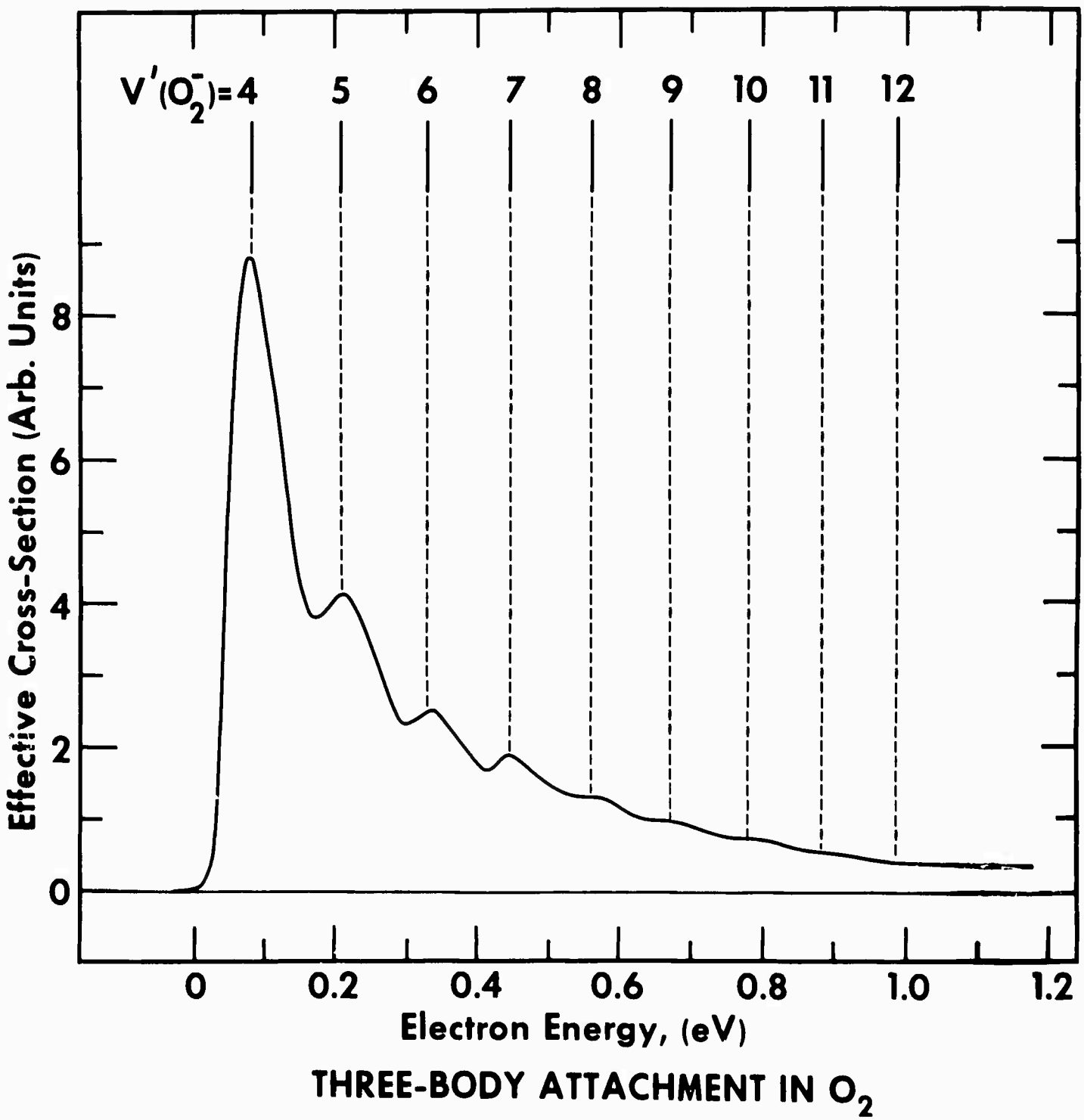
V'(O2-)=4
5
6
7
8
9
10
11
12
Effective Cross-Section (Arb. Units)
0
2
4
6
8
0
0.2
0.4
0.6
0.8
1.0
1.2
Electron Energy, (eV)
THREE-BODY ATTACHMENT IN O2

FIG. 3

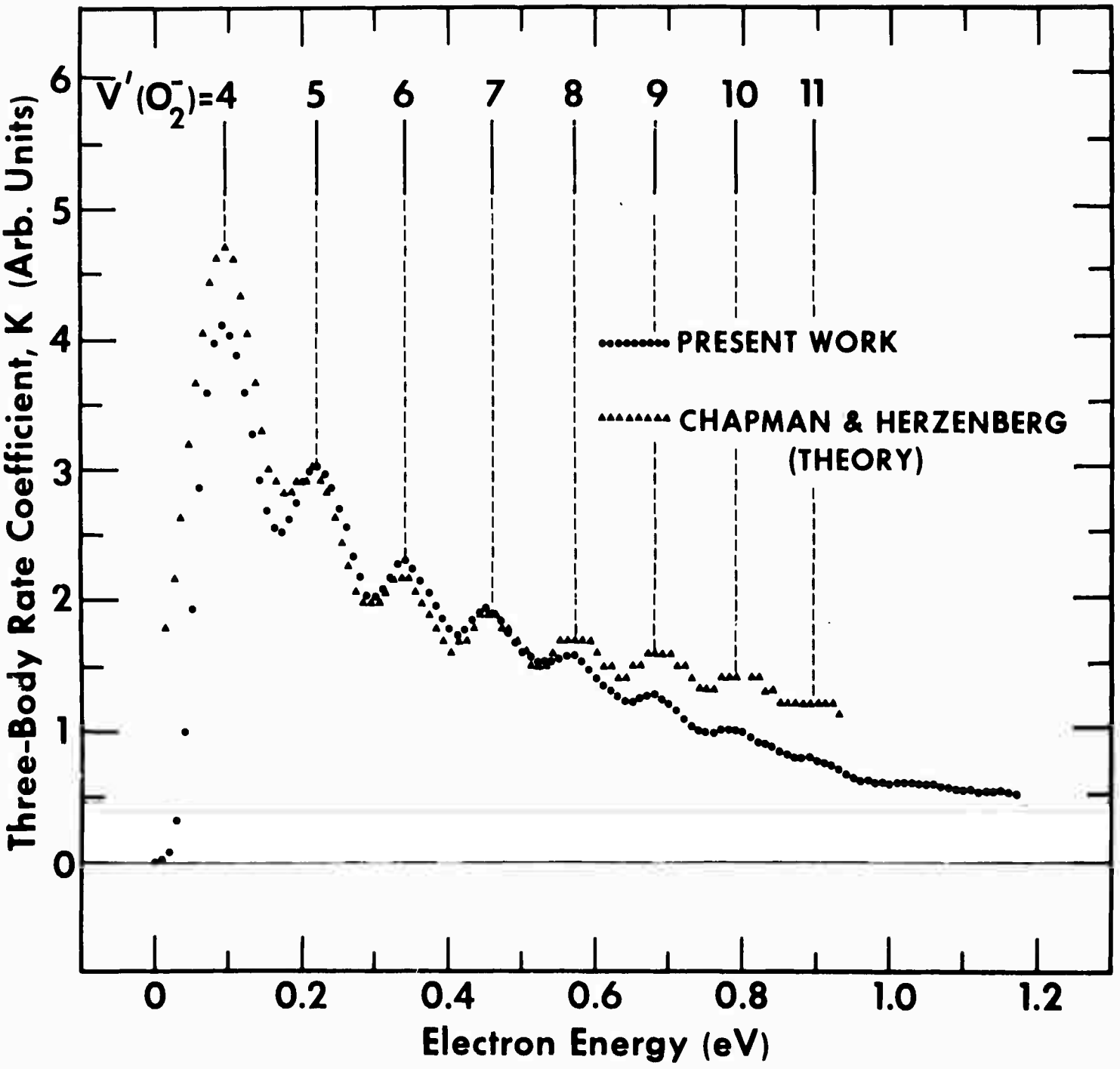

COMPARISON OF EXPERIMENTAL AND THEORETICAL THREE-BODY RATE COEFFIENT IN PURE O_2 AT ROOM TEMPERATURE

FIG. 4

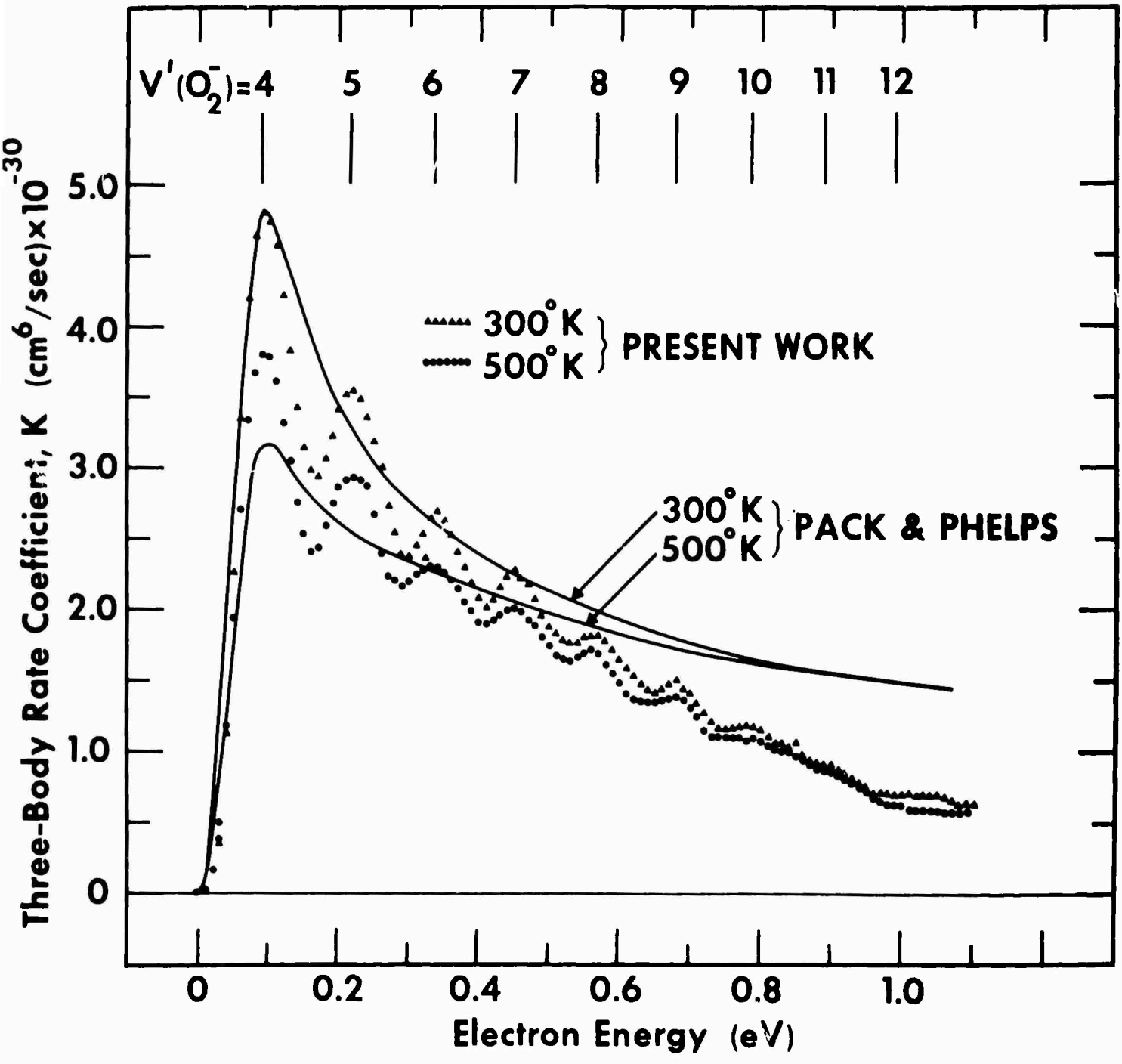

COMPARISON OF PRESENT DATA WITH SWARM EXPERIMENTS AT ROOM TEMPERATURE AND 500°K

FIG. 5

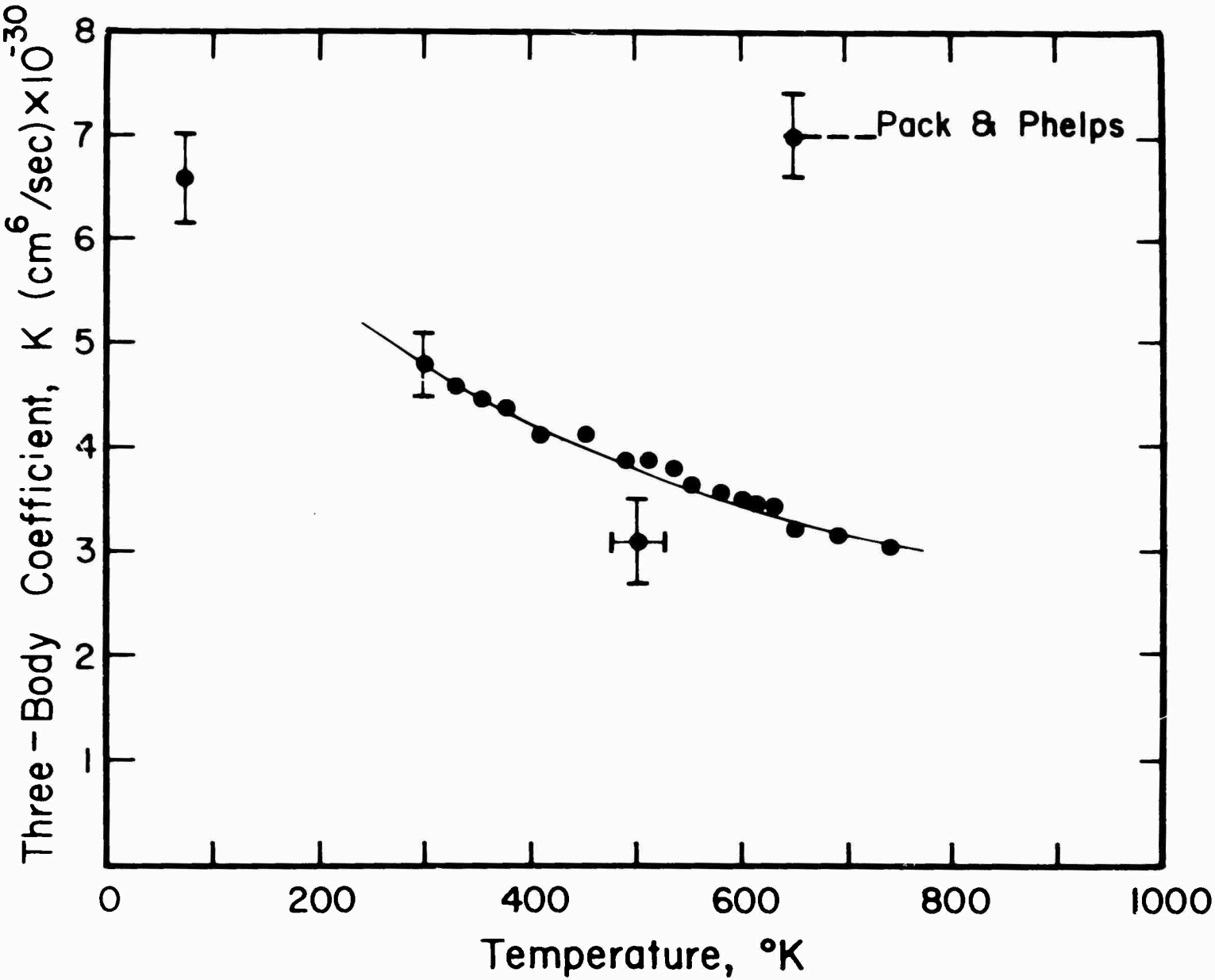

TEMPERATURE DEPENDENCE OF THREE-BODY ATTACHMENT IN O_2

FIG. 6

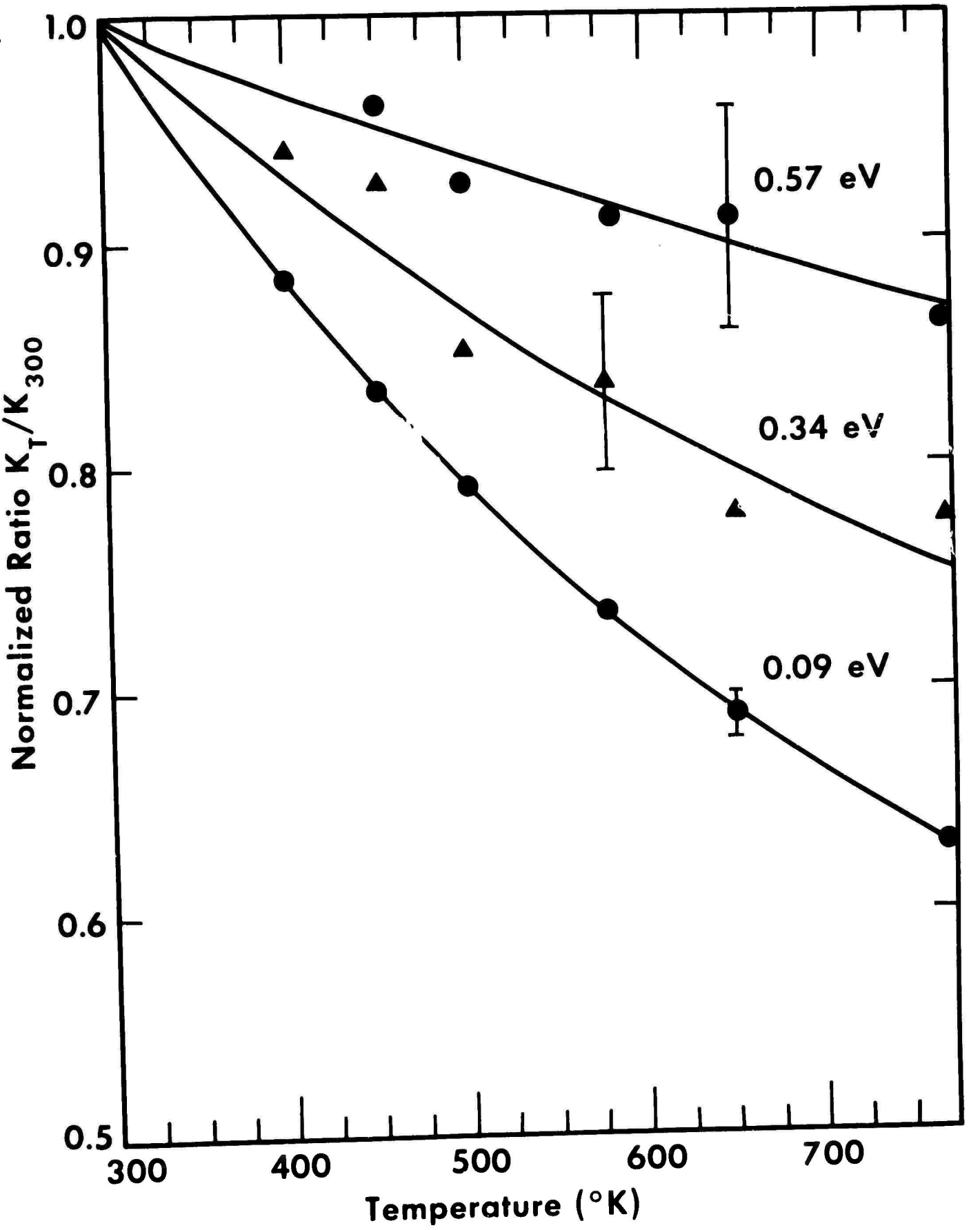

TEMPERATURE DEPENDENCE OF K AT VARIOUS ELECTRON IMPACT ENERGIES.

FIG. 7

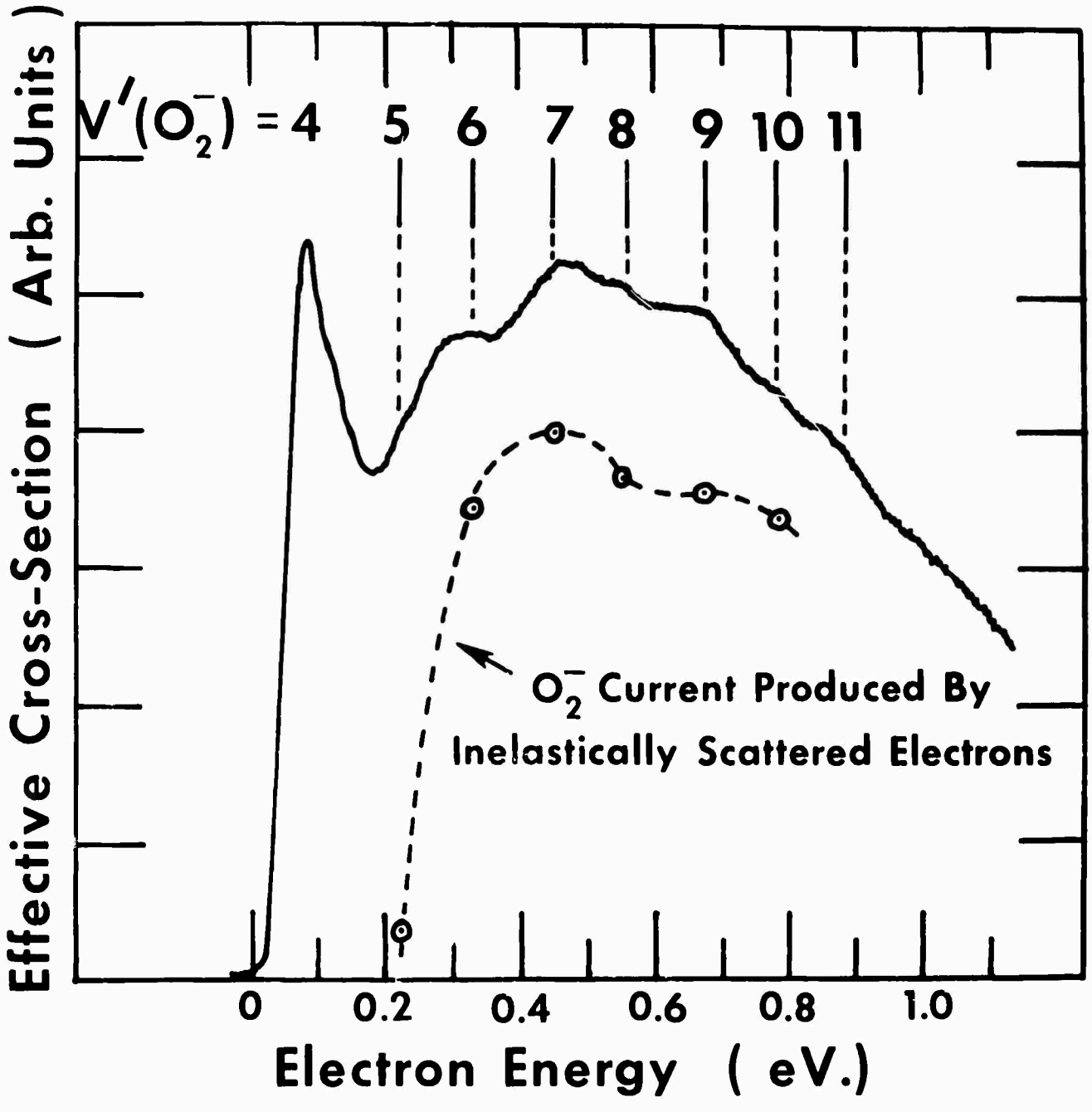

EFFECTIVE CROSS-SECTION FOR O_2^- PRODUCTION AT HIGH PRESSURE

FIG. 8

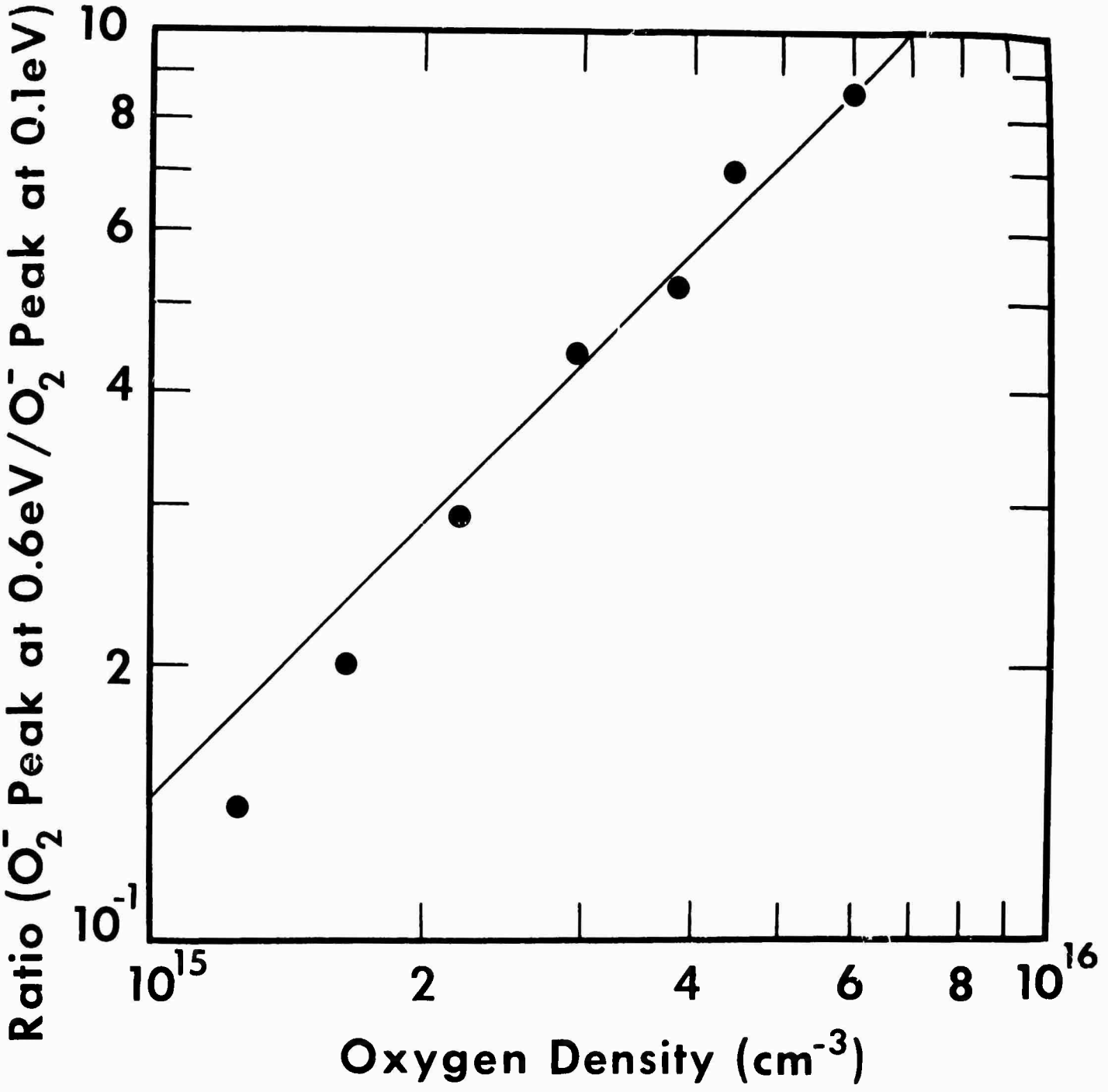

PRESSURE DEPENDENCE
(O_2^- PEAK AT 0.6eV/O_2^- PEAK AT 0.1eV)

FIG. 9